Dispersion-induced patterns

P. Coullet, T. Frisch, and G. Sonnino
Faculté des Sciences, Institut Non-Linéaire de Nice, Université de Nice Sophia-Antipolis, 06108 Nice Cedex 2, France
(Received 13 September 1993)

We propose a mechanism for pattern formation in spatially extended systems which generalizes the Faraday instability. We illustrate this by means of several examples ranging from mechanics to chemical oscillations.

PACS number(s): 47.20.Ky

Pattern formation has been widely studied both from the experimental and theoretical viewpoint [1]. All known forms of patterns come from a spontaneous symmetry-breaking phase transition, when a spatially translational-invariant state goes into a structured one. Patterns have been observed, for example, in convecting fluids, in liquid crystals, and in the buckling of elastic plates, etc. In such cases the selection of the wave number is induced by the geometrical constraints on the experimental system. In convecting fluids the wavelength of the pattern is comparable to the height of the container. However, there exists mechanisms for pattern formation which require neither external gradients nor a specific geometry. The appearance of such intrinsic patterns was first predicted theoretically by Turing [2] and only recently observed [3,4].

In this paper we describe another generic pattern-forming mechanism. It generalizes the Faraday instability of a free surface of a fluid subjected to a periodic vertical acceleration [5]. The wave number of the patterns, observed for the Faraday instability, depends on the forcing frequency. Patterns then arise as the interplay between dispersive waves and the parametric nature of the instability [6–9]. Our generalization will be illustrated by two simple physical systems. The first is a mechanical system, a chain of pendula parametrically pumped. The other example is an assembly of spatially distributed generic oscillators governed by a complex Ginzburg-Landau equation[10], subjected to a parametric forcing. The ensuing patterns observed resulting from the resonance between the frequency of excitation and the frequency of a standing wave will be called "dispersion-induced patterns." Finally, we shall present an application of the results obtained in the Ginzberg-Landau model to a simple autocatalytic chemical reaction.

As a first system, let us consider a chain of pendula in a periodically varying gravitational field close to twice the natural frequency of the pendulum. In the continuum approximation such a system is described by the equation

$$\Theta_{tt}+\delta\Theta_t+\{1+f\sin[2(1-\nu)t]\}\sin(\Theta)=\Theta_{xx}\ , \tag{1}$$

where δ, f, and ν represent, respectively, the damping, the amplitude of the forcing times the square of forcing frequency, and the detuning parameters. We shall show that a standing-wave pattern is excited, the wavelength of which is selected by the forcing frequency. The unforced, undamped system can sustain waves, the dispersion relation of which is given by $\omega=\sqrt{1+k^2}$. As usual in parametric resonance, the strongest response of the medium is subharmonic and is at one-half the frequency ω_f of the external forcing. It is then natural to expect a pattern with a wave number matching the frequency $\omega_f/2$ (Fig. 1). For the sake of simplicity, we shall only consider the case of weak damping, weak forcing, and weak detuning,

$$f=\epsilon f_0\ ,\quad \delta=\epsilon\delta_0\ ,\quad \nu=\epsilon\nu_0\ , \tag{2}$$

where $\epsilon\ll 1$. In such a parameter regime, we seek a solution of Eq. (1) of the form

$$\Theta=A(t)e^{it}+\overline{A}(t)e^{-it}+A_{\mathrm{HOH}}\ . \tag{3}$$

Here A_{HOH} involves corrections due to higher-order harmonics, A represents the amplitude of the oscillation, and $\overline{A}$ stands for the complex conjugate. At the leading order the equation for the amplitude reads as

$$A_t=-\mu A+i\alpha|A|^2A+i\beta A_{xx}+\gamma\overline{A}e^{-i2\nu t}\ , \tag{4}$$

where the following coefficients are derived from (1) using $\sin\Theta=\Theta-\Theta^3/6$: $\alpha=-\frac{1}{4}$, $\beta=-\frac{1}{2}$, $\gamma=f_0/4$, and $\mu=\delta_0/2$. After the transformation $A(t)\rightarrow A(t)e^{-i\nu t}$ we obtain

$$A_t=i\nu A-\mu A+i\alpha|A|^2A+i\beta A_{xx}+\gamma\overline{A}\ . \tag{5}$$

The stability analysis of the equilibrium state ($A=0$) of the chain is straightforward. Let us write the perturba-

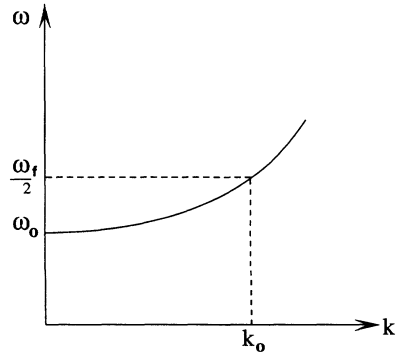

FIG. 1. The mechanism for wave-number selection is illustrated by means of the dispersion relation.

tion of the equilibrium state as $A=(X_k+iY_k)e^{\sigma t+ikx}$. The growth rate of such a perturbation then reads as

$$\sigma=-\mu\pm\sqrt{\gamma^2-(\nu_0-\beta k^2)^2}\ . \tag{6}$$

For positive detuning, we rediscover the usual parametric instability in which the instability sets in at zero wavelength. This result can be directly derived from (1) using properties of the Mathieu equation. However, for negative detuning, the instability sets in at a finite wave number $k^2=\nu_0/\beta$ when $\gamma>\mu$. Therefore, in this parameter range the pattern consists of a standing wave with a wave number proportional to the square root of the detuning (Fig. 2). The weakly nonlinear analysis is easily done by introducing an order parameter C for the amplitude of the oscillation in the following manner:

$$A=C(t)(X_k+iY_k)e^{ik_0x}+\text{c.c.}+A_{\text{HOH}}\ . \tag{7}$$

At the first order in the nonlinearity C obeys the following equation:

$$\frac{\partial C}{\partial t}=(\gamma-\gamma_c)C-\alpha^2\frac{9}{2\mu}|C|^4C\ , \tag{8}$$

where $\gamma_c=\mu$. The absence of a third-order term in (8) is due to the fact that the system we considered is quasiconservative.

For the second system, let us consider an assembly of spatially distributed oscillators subjected to a temporal parametric forcing with a frequency ω_f. The amplitude equation which describes the periodic modulation of such a system close to a Hopf bifurcation reads as [11]

$$A_t=(-1+i\nu)A+(1+i\beta)\nabla^2A -(1+i\alpha)|A|^2A+\gamma\overline{A}^{n-1}\ , \tag{9}$$

where n is defined by $\omega_f=n(\omega_0-\nu)$ and ω_0 is the natural frequency of the oscillators.

In (9) the distance from the threshold of self-oscillation, the damping coefficient, the nonlinear saturation coefficient, and the diffusion coefficient have all been rescaled to unity. The amplitude of the forcing is proportional to γ and the complex coefficient in front of the Laplacian measures dispersion. Now, consider the case $n=2$, which occurs when the forcing frequency is close to twice the natural frequency of the oscillators. The linear stability analysis of the nonoscillatory solution $A=0$ of (9) is straightforward. Setting $A=X+iY$ in the linearized equation, we obtain

$$X_t=(-1+\gamma)X-\nu Y-\beta\nabla^2Y+\nabla^2X\ , \tag{10}$$

$$Y_t=(-1+\gamma)Y+\nu X+\beta\nabla^2X+\nabla^2Y\ . \tag{11}$$

Let $X=X_ke^{ikx}e^{\lambda t}$ and $Y=Y_ke^{ikx}e^{\lambda t}$, then the equation for the eigenvalue λ reads as

$$\lambda^2+2\lambda(1+k^2)+c(k)=0\ , \tag{12}$$

where $c=(\nu-\beta k^2)^2-(\gamma-k^2-1)(1+\gamma+k^2)$. The first change of sign of an eigenvalue happens when $c=\partial c/\partial k=0$.

After some simple algebra one finds that the most unstable wave number k_0 and the instability threshold γ_c are given by

$$k_0^2=\frac{\beta\nu-1}{1+\beta^2}\quad\text{and}\quad\gamma_c^2=\frac{(\beta+\nu)^2}{(1+\beta^2)}\ . \tag{13}$$

Note that when $\beta\nu\to1$ the wave number at which the instability sets in tends to zero. Therefore, in the parameter regime such that where $\beta\nu>1$, the pattern is, as in the case of pendula, a standing wave, the wave number of which is selected by the linear instability (Fig. 3). Now consider briefly the amplitude of the pattern, setting

$$\begin{pmatrix}X\\Y\end{pmatrix}=e^{ik_0x}C(t)\mathbf{u}+\text{c.c.}+A_{\text{HOH}}\ , \tag{14}$$

in which $\mathbf{u}$ is determined by the linear analysis, we obtain close to the finite wavelength instability threshold

$$C_t=(\gamma-\gamma_c)\frac{(1+a^2)}{2|\beta|a}C-3(1+a^2)\frac{(\beta-\alpha)}{\beta}|C|^2C\ , \tag{15}$$

where $a=(\sqrt{1+\beta^2}-|\beta|)$.

Therefore, depending on the sign of the cubic term, in (15) the instability is either supercritical or subcritical. In the supercritical case, our numerical simulations have shown that the only stable solutions are the nontrivial

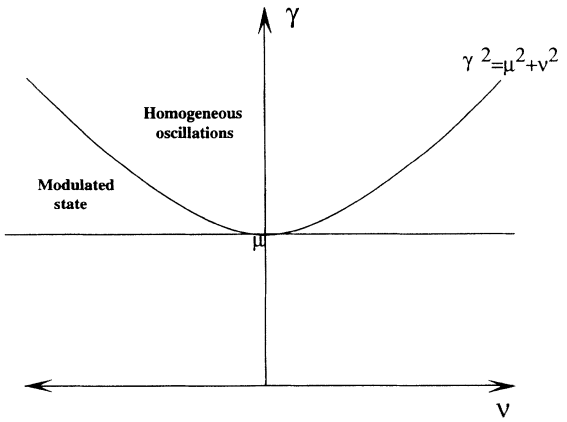

FIG. 2. The stability diagram for the chain of parametrically forced pendula.

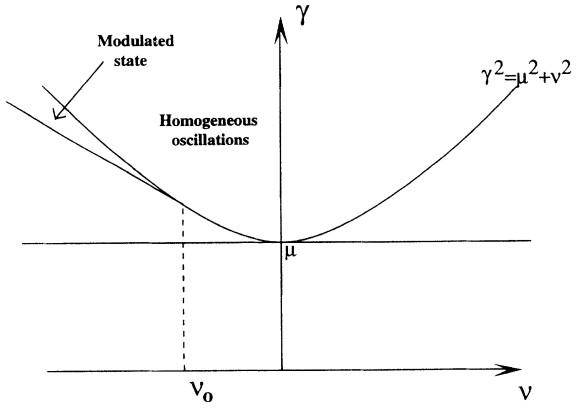

FIG. 3. The stability diagram for the Ginzburg-Landau equation where $\nu_0=1/\beta$.

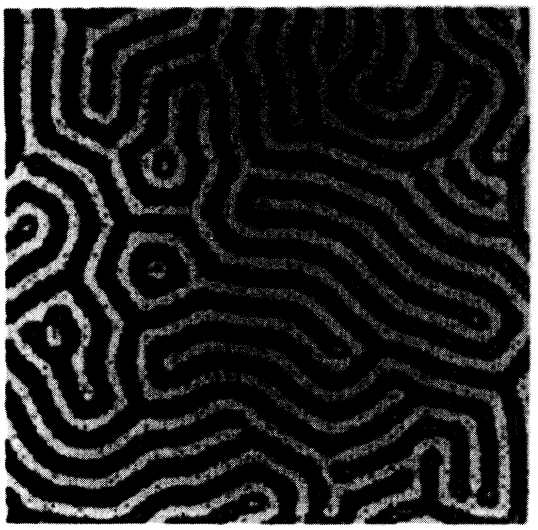

FIG. 4. Numerical simulations of the Ginzburg-Landau equation showing the real part of A. The pattern consists of rolls with different orientations. The numerical values are $\beta=-2.0$, $\nu=-2.0$, $\alpha=0$, and $\gamma=2.0$. The numerical simulations used a 256^2 grid and a finite-difference method (Gauss-Seidel-Crank-Nicholson) with $\delta x=0.5$ and $\delta t=0.005$.

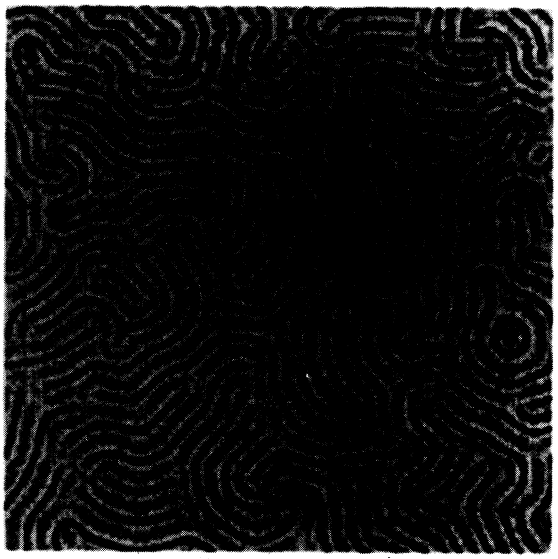

FIG. 5. Numerical simulations of the forced Brusselator equation showing the X variable. The pattern consists of rolls with different orientations [20]. The numerical values are $A=2.48$, $B=7.0$, $\gamma=0.206$, $\nu=0.61$, $a_1=1.0$, $a_2=0.5$, $a_3=1.2$, $a_4=0.3$, $D_x=1.0$, and $D_y=0.175$. Same numerical method as in Fig. 4.

homogeneous solutions (locked states) of (9).

For a two-dimensional (2D) system, a weakly nonlinear analysis of Eq. (9) shows that rolls are stable when the bifurcation is supercritical, and our numerical simulations confirm this fact (Fig. 4). For the 2D subcritical case our numerical simulations again have shown that the locked solutions are stable.

As an example of parametric forcing of dissipative oscillators, let us consider a parametrically forced autocatalytic chemical oscillation *below* the threshold of oscillations. This can be achieved, for example, by periodically flashing light on a photosensitive reaction [12]. For sake of simplicity, we choose the Brusselator model [13]

$$X_t = Ak_1 - (k_2 B + k_4)X + k_3 YX^2 + D_x \nabla^2 X \ , \tag{16}$$

$$Y_t = k_2 BX - k_3 YX^2 + D_y \nabla^2 Y \ . \tag{17}$$

Due to external forcing, the constants of reaction are periodically varying in time in the following way:

$$k_i = 1 + \gamma a_i \cos[(2A + \nu_1)t] \ . \tag{18}$$

We choose the time dependence of the parametric forcing to be close to twice the frequency of oscillation. In that case, conventional methods show that the envelope equation for the amplitude of oscillation is again (9) [14]. In the parameter region in which the instability set in at finite k_0, the pattern consists of a standing wave (Fig. 5). Therefore this standing-wave pattern is not a periodic modulation of a Turing structure [15] but a Faraday-like structure although the dispersion in the complex Ginzburg-Landau equation is proportional to the discrepancies in the diffusion constants. We emphasize that whatever the sign of $D_x - D_y$ is, the existence of dispersion-induced patterns depends only upon the sign of the detunning ν_1.

We have shown that dispersion-induced patterns appear in parametrically forced, mechanical systems and generic oscillators below the threshold of oscillation. Optic patterns can also be understood as a result of diffraction [16]. Experiments with two counterpropagating beams [17] display various patterns but cannot be interpreted within the general framework developed in this paper since they are not related to a parametric forcing. To end this paper, we note that adding terms oscillating at another resonant frequency in (17) may stabilize hexagons of the sort observed in the Faraday experiment [18]. Finally by playing with the relative phases between the forcings, more exotic patterns as, for example, quasicrystalline ones, may be stabilized [18,19].

It is a pleasure to thank S. Rica for stimulating discussions and C. Green and J. Montaldi for numerous suggestions. The work of G. Sonnino was sponsored by an EEC grant (Contract No. ERBSC1 CT005143). The financial support of E.E.C. grants (Contract Nos. SCI1 900800 and SC1 CT91-0683) is also acknowledged. Numerical simulations have been done on the Connection Machine of the Institut National de Recherche and Informatique et Automatique (INRIA) at Sophia-Antipolis through the R3T2 Network. The Institute Non-Linéaire de Nice is Unité de Recherche Associée du Centre National de la Recherche Scientifique No. 129.

[1] A. C. Newell, T. Passot, and J. Lega, Annu. Rev. Fluid Mech. **25**, 399 (1993).
[2] A. M. Turing, Philos. Trans. R. Soc. London Ser. B **237**, 37 (1952).
[3] P. de Kepper, V. Castets, E. Dulos, and J. Boissonade, Physica D **49**, 161 (1991).
[4] Q. Ouyang and H. L. Swinnyey, Chaos **1**, 411 (1991).
[5] M. Faraday, Philos. Trans. R. Soc. London **121**, 299 (1831).
[6] J. Miles and D. Henderson, Annu. Rev. Fluid Mech. **143**, (1990).
[7] S. Douady and S. Fauve, Europhys. Lett. **6**, 221 (1988).
[8] S. Ciliberto and J. P. Gollub, J. Fluid Mech. **158**, 381 (1985).
[9] A. B. Ererskii, M. I. Rabinovich, V. P. Reutov, and I. M. Starobinets, Zh. Eksp. Teor. Fiz. **91**, 2070 (1986) [Sov. Phys. JETP **64**, 1228 (1986)].
[10] A. C. Newell, *Lectures in Applied Math,* Vol. 15, *Non-Linear Wave Motion* (American Mathematical Society, Providence, 1974), pp. 157–163.
[11] P. Coullet and K. Emilson, Physica D **61**, 119 (1992).
[12] S. Muller (private communication).
[13] G. Nicolis and I. Prigogine, *Self Organization in Non-Equilibrium System* (Wiley, New York, 1977).
[14] G. Sonnino, T. Frisch, and P. Coullet (unpublished).
[15] P. Borckmans, G. Dewell, and A. de Witt, Physica A **188**, 137 (1992).
[16] L. A. Lugiato and R. Lefever, Phys. Rev. Lett. **58**, 2209 (1987).
[17] G. Grynberg, E. Le Bihan, P. Verkerk, P. Simoneau, J. R. R. Leite, D. Bloch, S. Le Boiteux, and M. Duclay, Opt. Commun. **67**, 363 (1988).
[18] W. W. Edwards and S. Fauve, C.R. Acad. Sci. Paris II **315**, 417 (1992); Phys. Rev. E **47**, R788 (1993).
[19] B. Christiansen, P. Alstrom, and M. T. Levinsen, Phys. Rev. Lett. **68**, 2157 (1992).
[20] In such a parameter regime, we have numerically checked that the homogeneous nonoscillating solution is stable in the absence of the parametric forcing.

FIG. 4. Numerical simulations of the Ginzburg-Landau equation showing the real part of A. The pattern consists of rolls with different orientations. The numerical values are $\beta=-2.0$, $\nu=-2.0$, $\alpha=0$, and $\gamma=2.0$. The numerical simulations used a 256^2 grid and a finite-difference method (Gauss-Seidel-Crank-Nicholson) with $\delta x=0.5$ and $\delta t=0.005$.

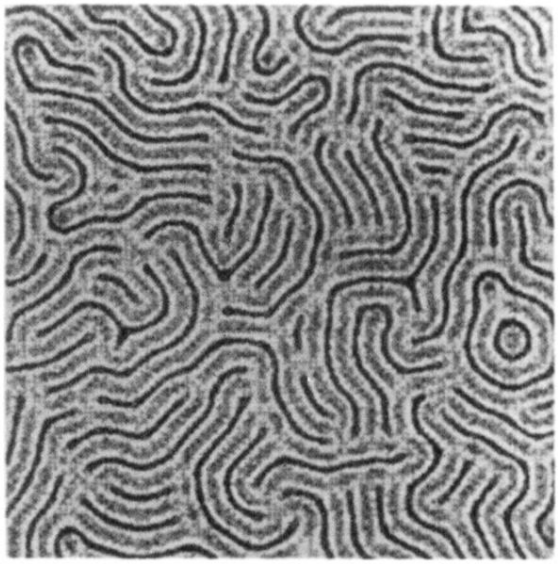

FIG. 5. Numerical simulations of the forced Brusselator equation showing the X variable. The pattern consists of rolls with different orientations [20]. The numerical values are $A=2.48$, $B=7.0$, $\gamma=0.206$, $\nu=0.61$, $a_1=1.0$, $a_2=0.5$, $a_3=1.2$, $a_4=0.3$, $D_x=1.0$, and $D_y=0.175$. Same numerical method as in Fig. 4.